

Review Article

RADIOLOGICAL ASPECTS OF HR-CT SCAN ON TEMPORAL BONE

Widiana Ferriastuti,^{ID} Ida Bagus Gede Ramayuda^{ID}

Department of Radiology, Faculty of Medicine, Universitas Airlangga/ Dr. Soetomo General Academic Hospital, Surabaya, Indonesia

ABSTRACT

The high-resolution computed tomography (HRCT) scan used in the 1980s offers a distinct advantage in interpreting images of the temporal bone. To obtain the right image reconstruction and to provide meaningful information, a certain degree of tilt is required, so that radiologists and clinicians can get more real imaging information on structural abnormalities in the temporal bone and its soft tissue constituents. The technique or protocol in HRCT of the temporal bone becomes an essential primary aspect in presenting the analyzed structure, the assessment of the small form of the auditory bones, the soft tissue of the inner ear and the cranial nerves that pass through the temporal bone structure is much easier to analyze with the help of reconstruction according to the HRCT protocol for temporal bone, yet the MRI is preferable for soft tissue evaluation. In the end, the standard structure, congenital abnormalities and pathological problems in the temporal bone structure can be identified and informed to the clinician as a step to determine further treatment.

Keywords: Radiological aspects; HR-CT Scan; temporal bone; congenital abnormality; illness

Correspondence: Widiana Ferriastuti, Department of Radiology, Faculty of Medicine, Universitas Airlangga/ Dr. Soetomo General Academic Hospital, Surabaya, Indonesia. E-mail: widiana_ferriastuti@yahoo.com

How to cite: Ferriastuti, W., & Ramayuda, I.B.G. (2022). Radiological Aspects of HR-CT scan on Temporal Bone. Folia Medica Indonesiana, 58(1), 88-102. <https://doi.org/10.20473/fmi.v58i1.23836>

pISSN:2355-8393 • eISSN: 2599-056x • doi: 10.20473/fmi.v58i1.23836 • Fol Med Indones. 2021;58:88-102
 • Submitted 22 Nov 2021 • Revised 2 Jan 2021 • Accepted 21 Feb 2021 • Published 5 March 2022
 • Open access under CC-BY-NC-SA license • Available at <https://e-journal.unair.ac.id/FMI/>

Hi i j i i j t u r

1. High-resolution computed tomography (HRCT) scan has advantage for best image reconstruction and informative in interpreting images of the temporal bone.
2. The essential primary aspect in HRCT of the temporal bone scan is technique and protocol.

INTRODUCTION

High-resolution computed tomography (HRCT) is a type of commonly used CT scan with a special technique to increase the resolution or sharpness of the CT image, with a cut thickness of about 0.625-1.25 mm reconstructed with a high algorithm using a bone algorithm. Using a scan time of 0.5-1 second, with a power of 120 kV, 100-200 mAs is required with collimation of 1.5-3 mm, a matrix size of 768 x 768 or its largest resulting in better imaging (Shaffer et al. 1980; Torizuka and Hayakawa 1992).

OVERVIEW

HR CT technique of the temporal bone

Currently, there are two techniques for taking CT of the temporal bone, namely MSCT (Multi-Slice CT) which is commonly used, and CBCT (Cone Beam CT) which have started to take over the role of MSCT. CBCT uses a rotating gantry, where the x-ray tube and the detector touch. The conical x-ray beam is directed

directly through the middle portion of the temporal bone towards the two-dimensional detector. Since CBCT uses a two dimensional FOV detector, only one 360 degrees rotation of the gantry produces 3-dimensional data. 110 kV, ± 140 mAs, field of view 15x5 cm high resolution, slice thickness 0.15 mm, scan time 40 s is a parameter that becomes a reference protocol for scanning with CBCT (McCullough & Zink 1999).

The resulting MSCT image is obtained from a single image plane using a multi-slice detector. Patients only need to lie in the gantry without a specific marker and then the radiologist just follow the image parameters according to the machine with the following parameters: 120 kV, 250 mAs, collimation 0.5 mm or 0.625 mm and scan time 1.0 s. After completing the process, the data was processed almost similarly to CBCT, reconstructed with 1 mm thickness using ultra high-resolution mode. The technician was instructed to make a parallel reconstruction with the semicircular lateral canal to produce an axial cut, while the coronal

cut was reconstructed right on the perpendicular perpendicular to the axial. The most anterior coronal section is directly anterior to the geniculate ganglion of the facial nerve. This procedure is applied to both the right and left temporal bones, using a window depth of 4000 HU and a window level of 200 HU, which actually depends on the convenience of the radiologist which makes it easier to see and analyze the stapes and suspensory ligaments in the middle ear cavity (McCullough & Zink 1999).

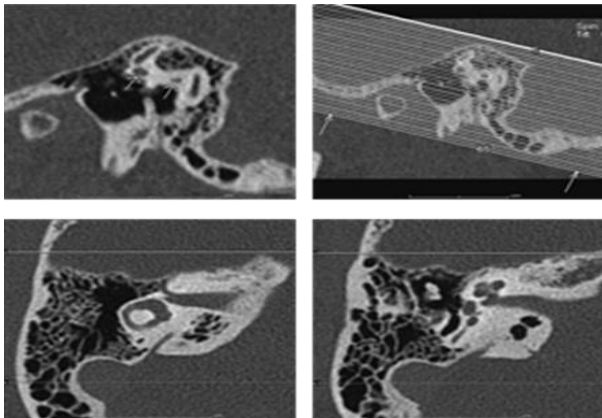


Figure 1. Creation of standard axial and coronal CT scan data of temporal bones

Note: (a) after the data source has been obtained in three dimensions (3D) on the scanner console, image is sagittal and then scrolled to obtain an image of the anterior and posterior limb canal semicircularis lateralis (short white arrows). (b) make axial cuts by setting overlapping parallel lines with a distance of 0.1 mm. (c) if the axial reconstruction is correct, it will reveal the entrance of the lateral semicircular canal. (d) when scrolled, it showed cochlear fossette, modiolus and footplate stapes that are outlined.

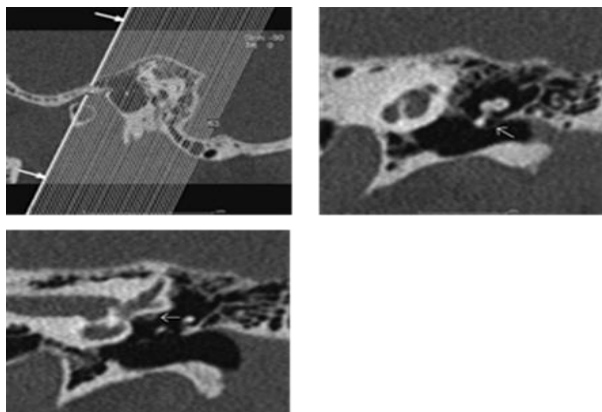


Figure 2. The coronal reconstruction is made in the same steps as the axial cut, so that the finished coronal cut could show Prussak's space (short white arrow) and facial nerve canal (white arrow in the last image) clearly

Temporal bone anatomy

The temporal bone is located on the lower side of the cranium base. It is located on the lateral side of the temporal lobe of the cerebral, consisting of five bones that compose it, among others: squamous, petrous, mastoid, tympanic, styloid processus. Inside the

temporal bone, there are several essential ear structures, namely middle and inner ear. The lower part of the temporal bone is also a part of the joint with the mandibular bone which forms the temporomandibular joint (Graham et al. 2000).

Ear anatomy

The ear consists of three parts; outer, middle and inside. This section detects, delivers and converts sound signals into electrical stimuli that are transmitted by afferent auditory nerve fibers to the central nervous system.

Outer ear

The outer ear has a canal \pm 3 cm in length, where 1/3 laterally is on the cartilage, while 2/3 inside is hard bone. This canal narrows and curves to protect the tympanic membrane from foreign objects and direct trauma. Innervated by n. auriculotemporal (n. trigemine), n. plexus cervicalis, n. vagus and n. facialis. In acoustic neurinoma patients, cough reflex originating from n. vagus disappears (Hitselberger's sign) (Park et al. 2000).

Middle ear

Middle ear consists of several components, namely cavum tympanic, temporal bone pneumatic system, and Eustachian tube. The tympanic cavity and the pneumatic system are aerated from eustachian tube can open in the nasopharynx. The outer ear canal and tympanic cavity are separated by eardrum which forms a 55 degree angle with the ear canal on the hard bone (Swartz & Harnsberger 1998).

The middle ear cavity is divided into three parts based on the level of the tympanic membrane. The level above tympanic membrane consists of the epitympanic recess of the attic with the head of malleus os, the incus body and the ligament and muscle folds which then pocket together with the chorda tympani. The level of the tympanic membrane consists of the mesotympanum, while the level below the tympani membrane consists of the hypotympanic recess. Between epi and mesotympanic anatomically, some constructs allow retention of secretions during inflammation and lack of aeration in the attic. This causes chronic epitympanitis and cholesteatoma. The pneumatization of temporal bone varies widely. The pneumatization system is well-developed that extends to both occipital and zygomatic arch regions. Formation of the mastoid process begins after birth between the second or the fifth year, and the process is complete at the age of 6-12 years. In this area, aeration blockage during childhood will result in repeated inflammation of the middle ear. This inflammation can have more severe complications in the future (Hasso et al. 1996, Park et al. 2000).

Ossicles

Originating from the inner surface of the tympanic membrane to the oval window, there are interconnected bony bones that can still move, called as ossicles.

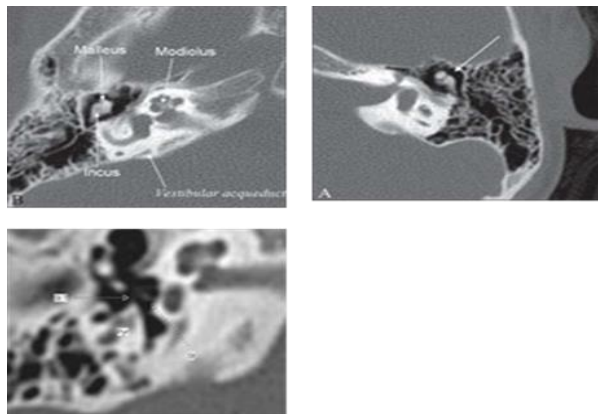


Figure 3. (a) Left axial CT scan temporal showing incus and malleus. (b) right axial CT scan cut temporal showing association with modiolus and vestibular aquaduct (white arrow). (c) bone stapes (white arrows)

Eustachian tube

The Eustachian tube is a link between middle ear and nasopharynx. Its function is to balance the pressure passing through tympanic membrane. Contraction of tensor veli palatine and salpingopharyngeus outer side of tympanic cavity dilates and opens the eustachian tube.

Inner ear innervation

The horizontal portion of the facial nerve passes through the tympanic cavity in the labyrinth wall in the bony canal just superior to the footplate of the stapes—Chorda tympani, branches that return from the facial nerve before exiting through the stylomastoid foramen. The chorda tympani enters the middle ear after leaving the bony canal and passes through the medial side of the neck of the malleus bone, then fuses to the carotid wall. The chorda tympani supplies the submandibular and sublingual glands as well as the anterior 2/3 of the tongue. Sensory information about the tympanic canal (middle ear) is carried by multiple nerves that form the tympanic plexus at the promontory in the medial wall.

Inner ear

The inner ear, also known as labyrinthine cavity, functions to transmit sound to the central nervous system as well as assist balance. Auditory transduction, converting mechanical energy into electrochemical, occurs in the cavity of the labyrinth. The labyrinth cavity is essentially made of a labyrinthine membrane surrounded by bones. Labyrinth bone is a series of bony cavities inside the temporal bone. The labyrinth

membrane is the membrane sacs and channels that are connected inside the labyrinth bone. The labyrinthine membrane is surrounded by perilymph and contains endolymph. The labyrinthine membrane also has cochlear, vestibular and semicircular components.

What to report on the examination of the temporal bone?

The format of reporting the results of the HRCT examination of the temporal bone has been widely discussed in articles circulating at this time. We tried to present a quite complete format, including structural assessments and possible things that clinicians need, including identity, date of examination, previous examination for comparison, clinical indication for HRCT examination of temporal bone (Graham et al. 2000, McCollough & Zink 1999).

At each examination of the temporal bones, either right or left were assessed: External auditory canal, mastoid complex, middle ear covering; whether the bone ossicles and pneumatization were normal, the tympani tegmen and scutum were normal, the oval and round window were standard, the inner ear included cochlea, vestibule, semicircular canal and internal auditory canal were normal, the vestibular aquaduct was not enlarged, the passage and caliber of the facial nerves, including the mastoid pars were normal, the internal carotid artery and jugular veins travelled normally (McCollough & Zink 1999, Swartz & Harnsberger 1998).

Congenital abnormalities

Congenital abnormalities of the outer ear

Earlobe

Malformation of the earlobe can affect the size, shape, position and orientation of the pinna (auricle). The complete absence of pinna (anotia) may occur. Various classification schemes have been proposed to assess the severity or deformity (Weerda 1988).

Table 1. Classification of ear lobe malformations

Dysplasia class	Characteristic
Class I (mild malformation)	Most of the structures resemble normal ear lobe.
Class II (moderate malformation)	Some structures are still normal, when the operation requires additional skin or cartilage tissue
Class III (severe malformations)	There was no visible structure of the normal earlobe

External auricular canal

Failure to recanalize the first cleft tissue can lead to malformation of external auricular canal (Ko'sling et al. 2009, Mayer et al. 1997). The absence of a meatal opening below the tragus indicates complete aural atresia. Atresia or incomplete stenosis should be



suspicious if the pinna is abnormal and the external auricular canal diameter is less than 4 mm or the tympanic membrane cannot be visualized (Chandrasekhar et al. 1995).

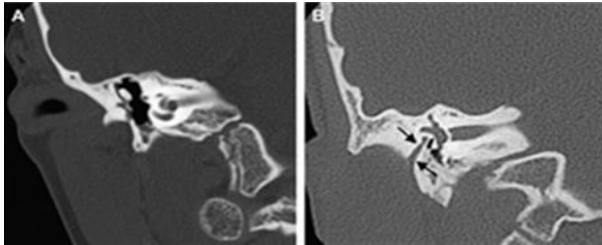


Figure 4. (a) coronal cut CT scan of the right temporal bone at the level of the cochlea showing total atresia of the external auditory canal. (b) coronal CT scan of the right temporal bone more posteriorly at the level of the vestibule showing a short and shallow short and shallow facial nerve segment

First branch cleft anomaly

This occurs as a result of the abnormal ectodermal closure of the gap. It usually occurs along the baseline of the auricular canal external to the submental area. These disorders can occur as preauricular cysts, sinus or recurrent external otitis (Yalcin et al. 2003).

Congenital cholesteatoma

Congenital cholesteatoma occurs more frequently in the middle ear. Children with atresia canalis auricular externa can develop cholesteatoma (either primary or secondary) at the site of stenosis or deep into the attic plate (Johnson et al. 1983).

Congenital abnormalities of the middle ear

Malleus

These include aplasia, fixation of incudomaleolar joint, fusion of the malleus head to the long process of the incus head and stapes (triple bony union). A rare malleus anomaly is congenital fixation. From the head of the malleus to the lateral epitympanic wall called as malleus bar.

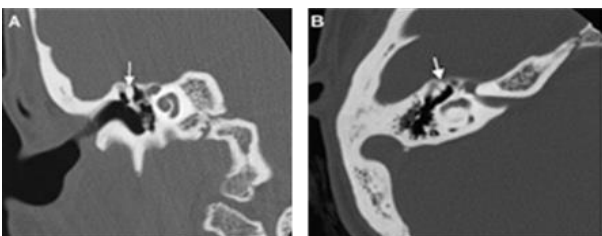


Figure 5. (a) coronal CT scan of the right temporal bone showing attached malleolus bone fixed superolateral to the epitympanic wall. (b) same axial temporal CT scan section

Incus

Abnormalities including aplasia, long processus deformity, fusion of the short processus incus to the lateral semicircular canal and fibrous fusion of the incudostapedial joint or joint absence.

Stapes

These included absent stapes superstructure, aplasia, stapes head abnormalities, monopod stapes, fixation of the stapes head to the promontorium, and footplate fixation.

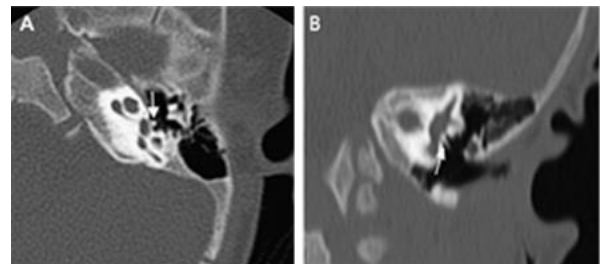


Figure 6. monopod stapes. (a) axial slice and (b) coronal reformat section of tempo CT scan left ear which shows single stapes called as monopod stapes

Other anomalies in the middle ear included persistence of the stapedia artery, absence of the stapedius muscle. Congenital cholesteatoma is identified as a whitish mass behind an intact tympanic membrane (Johnson et al. 1983).

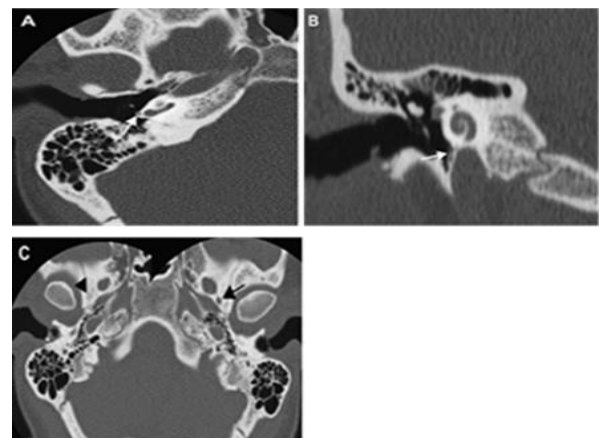


Figure 7. Persistent stapedia artery

Note: (a) axial section and (b) coronal section CT scan of the right temporal bone showing the canal still at the level of the promontory cochlea indicated by arrows. (c) on further examination, it was found that there was no normal foramen spinosum on the right side which was shown by the arrowhead when compared to the left side.



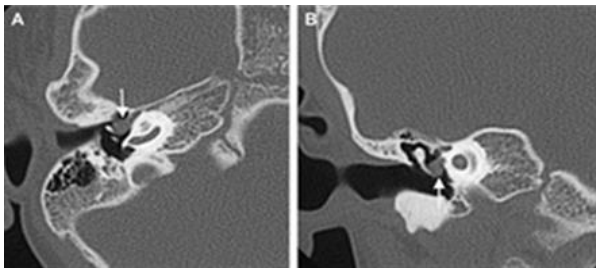


Figure 8. Congenital cholesteatoma. (a) axial section and (b) coronal section CT scan temporal showing rounded soft tissue with a flat edge in the middle ear space

The tympani cavity

Congenital abnormalities were hypoplastic, aplastic or extracavitation, and it was an extra cavity in an improper place.

Mastoid pneumatization

There might be normal, reduced or even non-pneumatized formation of the mastoid.

Congenital abnormalities of the inner ear

Malformation of the inner ear occurred as a result of disruption at embryogenesis stage. A newer classification had been proposed by Sennaroglu and colleagues (Sennaroglu & Saatci 2002).

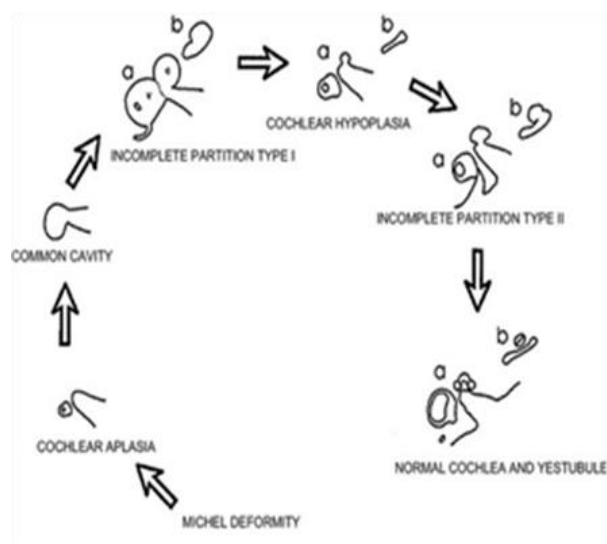


Figure 9. A schematic of a different degree to the development of the inner ear wherein the letters a and b represent successive stages that pass through the internal auditory canal and round window

The basis of this classification was embryological growth, but it also distinguished between classic Mondini and pseudo-Mondini abnormalities.

Michel deformity or labyrinthine aplasia

In this malformation, there was a complete labyrinthine aplasia to the point, where cochlear and vestibular elements are not formed. Due to the failure of the development of the otic vesicles to the absence of the formation of inner ear, this anomaly is described as an otocytic deformity and described as the extremely rare and the most severe inner ear abnormality (Quirk et al. 2019).

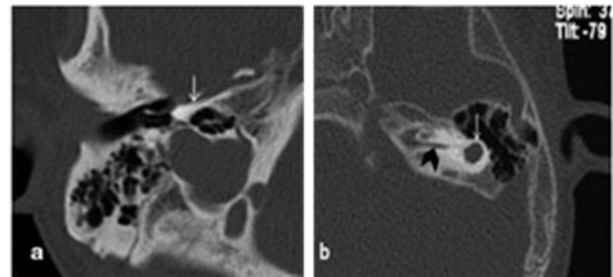


Figure 10. Michel Deformity (a) arrow shows no labyrinthine in small and dense otic capsule (b) white arrow shows rudimentary otocyst with narrowed internal auditory canal (black arrow)

This deformity occurs after the formation of the otic vesicles is complete, because the semicircular canal is the first structure to be formed from the otic vesicles. It is possible that the inner ear presents some rudimentary abnormalities of the semicircular canal. Failure to differentiate the promontory cochlear from associated labyrinthitis. A similar condition can occur after the condition of meningitis, where the formation of connective tissue and changes in the bone structure of the inner ear, including the cochlea take a place (Swartz & Harnsberger 1998).

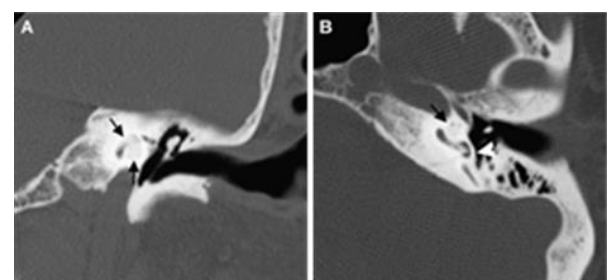


Figure 11. Labyrinthitis ossificans. (a) coronal slice and (b) axial cut CT scan of left temporal showing ossification of the middle groove and left apical cochlea of ossification labyrinthitis (black arrow), while the head of the white arrow indicates a normal cochlear promontorium Labirinitis

Cochlear aplasia

This malformation takes the form of the complete absence of cochlea. The vestibule, semi-circular canal and internal auditory canal are still present and normal, and sometimes hypoplastic.

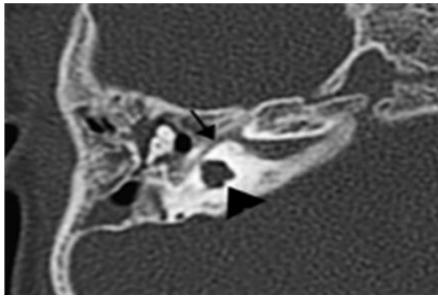


Figure 12. Cochlear aplasia. Shaped axial CT scan of right temporal showing absence of cochlea, arrowhead showing dysplastic right vestibule. There was also a mild right facial nerve abnormality indicated by the arrow activation mechanism

Common cavity deformity

Common cavity malformations in the form of cystic, cochlear fusion, vestibule and semicircularis canal including size variations. This disorder is often associated with narrowing or widening of internal auditory canal and dysplasia canalis semicircularis (Graham et al. 2000).

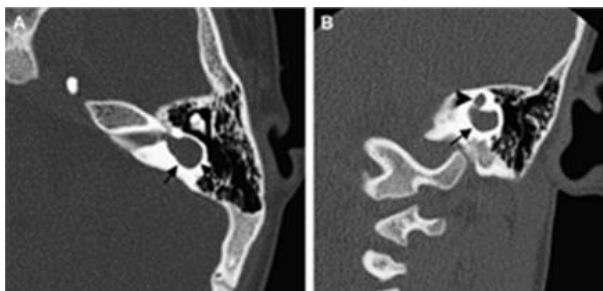


Figure 13. Common cavity malformations showed axial section (a), and coronal section CT scan of right temporal showing incomplete structures of the vestibule, cochlea and semicircular canal (b)

IP type I: Cochleovestibular cystic malformations

Distinguished for more clearly malformations between Pseudo-Mondigi (IP I) and classic Mondigi (IP II) by Sennaroglu and colleagues in 2002.

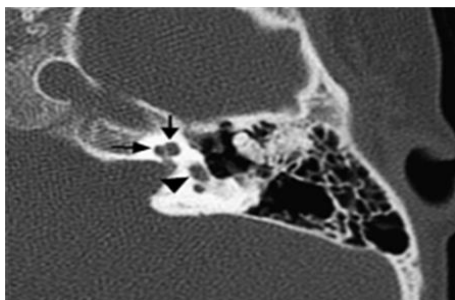


Figure 14. IP type I (number eight "8" malformation). On the axial CT scan the right temporal scan shows the cystic-shaped coclea (arrowhead) and vestibule (arrow) with no internal structures

abnormalities, the cochlear dimensions and vestibule are normal but have architectural defects in them. Cochlea is without a modiolus and looks cystic with a dilated vestibule without internal structure (Graham et al. 2000).

Cochlear hypoplasia

This deformity indicates a hypoplastic anomaly that is not even formed at all.

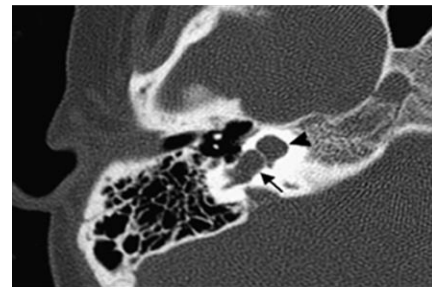


Figure 15. Cochlear hypoplasia. Axial cut CT scan of the left temporal showing cochlea that looks small (arrowhead) and vestibular (arrowhead)

IP type II: Classic mondini deformity

This malformation is in the form of a cochlea that rotates 1.5 times from the normal 2.75 turns. Interscalar defect occurs between the middle and apex rotation, where it coalesces into 1 space. Compared to IP I, type II is more common. Having a basal cochlear modiolus in type II, the incidence of meningitis is lower, and the likelihood of restoration of hearing with implantation is better (Graham et al. 2000).

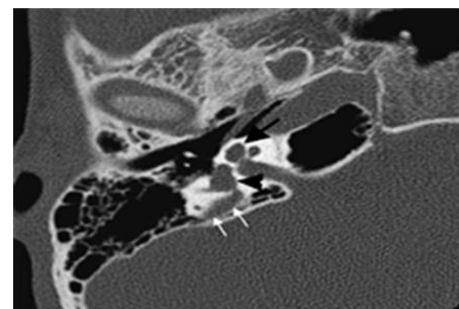


Figure 16. IP type II (Mondini malformation) Shown in the right axial CT scan of the right temporal showing the joining of the middle and apical grooves of the cochlea (black arrow). Large visible vestibule (arrowhead) and also visible widening of the vestibular aqueduct (white arrow)

Vestibular malformations

Independent vestibular abnormalities are very rare, usually co-occurring with IP I, IP II disorders and cochleovestibular hypoplasia. Semicircularis canal malformations include; dysplasia canalis semicircularis lateralis, common crus anomaly, and other anomalies such as CHARGE and BOR syndrome.

Dysplasia of the lateral semicircularis canal; is the most common disorder in the form of a short lateral semicircularis canal, with a wide and fused vestibule with common cavity, the superior and posterior semicircularis canals appear in normal proportions. Common crus anomaly, the posterior and superior semicircularis canals may widen and merge with the vestibule and common crus may not develop properly.

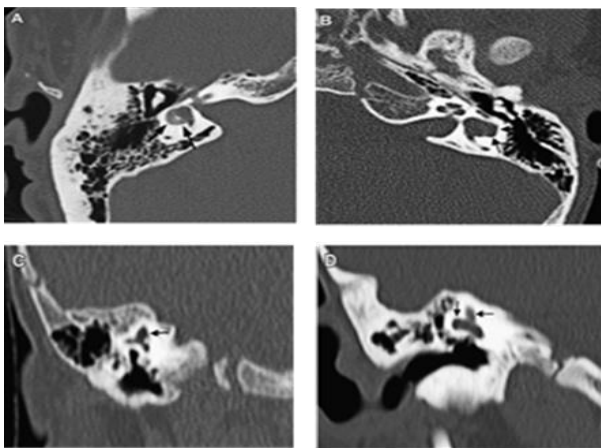


Figure 17. Dysplasia of the semisircularis superior canalis

Note: (a) axial CT scan of the right temporal showed shortening of the lateral semicircularis canal (arrow) suspected to be associated with mild dysplasia, (b) axial CT scan of left temporal in a different patient showed left vestibular dysplasia and left lateral semicircularis canal fused to form a common common. cystic cavity (arrow), (c) coronal cut CT scan of the right temporal showing dysplastic and enlarged right semicircular common crus canals posteriorly and superiorly (arrows), and (d) coronal cut CT scan of the right temporal showing similar abnormalities.

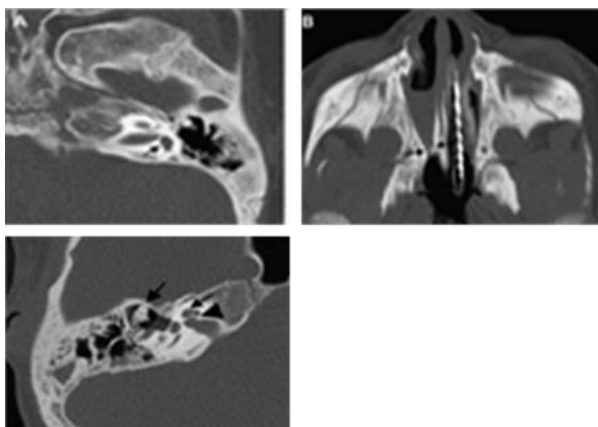


Figure 18. CHARGE syndrome

Note: (a) axial cut CT scan of the left temporal showing the absence of all semicircular canal structures with mild dysplasia of the left vestibule (arrow), (b) axial CT scan at mid-face level showing right choanal atresia, (c) Branchio-auto-renal syndrome. Axial cut CT scan of the right temporal showing hypoplastic indentation of the apical coclea (small arrow). Invisible cochlear modiolus was suspected of hypoplasia (arrowhead). Also, there was a short, calcified superior ligament located more anterior to the middle ear bony bones (Propst et al. 2005)

Other semicircularis canal abnormalities; CHARGE anomaly, is the total absence of the semicircularis canal. Meanwhile, BOR syndrome is an autosomal dominant disorder affecting the EYA 1 gene on chromosome 8 which is characterized by branchial fistulas and cysts, ear abnormalities that cause deafness, kidney malformations, inner ear abnormalities including cochlear hypoplasia, lateral semicircularis canal hypoplasia and cochlear aquaduct enlargement. and vestibular (Propst et al. 2005).

Enlarged vestibular aquaduct

This disorder is one that often occurs in middle ear malformations. It was reported in a study that enlarged vestibular aquaducts were probably associated with cochlear malformations in 76% and vestibular malformations in about 40% in each case (McElveen et al. 1997).

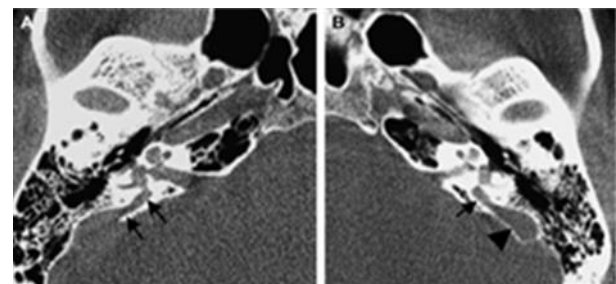


Figure 19. Syndrome of enlarged vestibular aquaduct

Note: (a) right axial section, (b) left axial section Temporal CT scan showed bilateral enlargement of the vestibular aquaduct (arrow) and prominent endolymph sac (arrowhead) (McElveen et al. 1997).

Internal auditory canalis stenosis

Rare disorder, where internal auditory canal diameter is <2 mm, and it is usually associated with narrowing of the cochlear nerve canal.

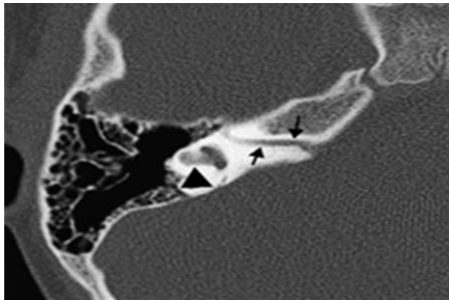


Figure 20. Refinement of the internal auditory canal. Right temporal CT scan axial cut showed narrowing (arrow). The patient also had a dysplastic vestibule and partially visible semicircularis canal (arrowhead)

Anomaly related to the X chromosome

It is a rare condition characterized by dilatation of the bulb of lateral end of the internal auditory canal. This disorder is associated with sensory deafness, and the risk of cerebrospinal fluid bursting at cochleostomy period (Phelps et al. 1991).

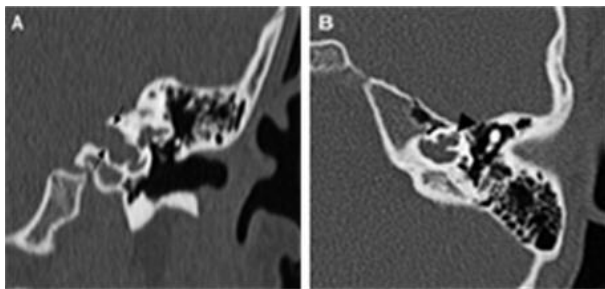


Figure 21. X chromosome anomaly

Note: (a) coronal cut, and (b) axial cut CT scan of left temporal showed abnormally dilated internal auditory canal (arrow) with dysplatic cochlea (arrowhead) accompanied by absence of cochlear modiolus

Figure of inflammation and infectious disease on CT scan of the temporal bone

Suspicion of inflammation and infectious disease in the temporal bone is the main indication for HRCT examination (Howard et al. 1990).

Outer ear

Acute otitis externa or swimmer's ear

The most common infection is characterized by pain, redness, swelling, often with conductive hearing loss when external auditory canal is obscured by this situation. These acute conditions are obstacles to CT scan examination.

Usually, the images showed things that were still normal, but it could be different if the clinical showed recurrences; or there were situations that underlied the abnormality, such as benign or malignant lesions (Swartz & Harnsberger 1998).

Chronic external otitis

CT scan imaging provides a good overview of the anatomical details behind obstruction by this chronic situation, including the extent and extent of bone erosions resulting from infection. Chronic inflammation results in subepithelial infiltration leading to fibrosis and stenosis of the external auditory canal (Hasso et al. 1989).

Malignant otitis externa

Demonstrated otorrhea and severe otalgia in both diabetic and immunocompressed patients. This condition is also related to a history of trauma. On physical examination, there is granulation tissue in the external auditory canal inferiorly, along the junction of the bone and cartilage. The infection spreads to the inferior side to the soft tissues and the temporomandibular joint (Howard et al. 1990). Malignant otitis externa has been classified according to its grade, namely Grade I: pinching of the external auditory canal with and without facial nerve paralysis, Grade II: extension to the superior, skull base osteitis, and/ or involving multiple cranial nerves, and Grade III: extension to the temporal or intracranial bone and involves the contralateral.

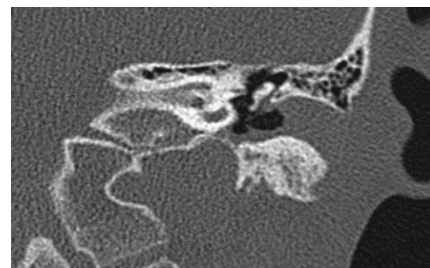


Figure 22. Left temporal CT corona-cut scan showed soft tissue filling the external auditory canal in a diabetic patient with Grade I (pinching) malignant otitis externa. Thickened tympanic membrane

Middle Ear

Acute otomastoiditis and its complications

manifested clinically as ear pain, fever, and redness of the tympani membrane. The middle ear and mastoid are generally exposed to expansion of infection from upper respiratory tract and bacteria enter through \eustachian tube. Temporal CT scan can show an image of ossicular erosion, destruction of the middle



ear which resembles an aggressive tumor accompanied by lymphadenopathy.

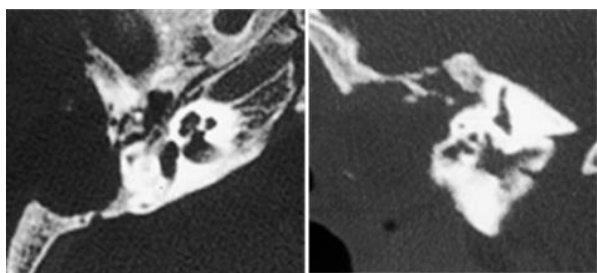


Figure 23. Tuberculous otomastoiditis with parenchymal abscess. (a) axial section (b) coronal cut CT scan right temporal showing middle ear destruction

Coalescent mastoiditis

A temporal CT scan is performed if there is suspicion of non-specific debris which is indicated by the presence of multiple air fluid levels. A temporal CT scan will show the condition of mastoid septa, ossicular chain, cortex outside and inside the mastoid bone.

In this clinical patient, the important point was that when mucoperiosteal disease became a bone disorder with enzymatic absorption of the mastoid bone septa and the development of intramastoid empyema, it led to a coalescent mastoiditis condition (Hasso et al. 1989).

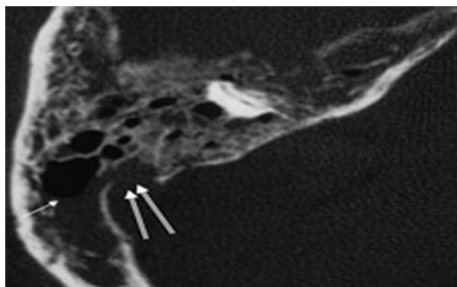


Figure 24. Acute coalescent mastoiditis. Right temporal CT scan axial section showed extensive mastoid debris with air fluid level (arrow). All septa are thin and irregular. There is also a sigmoid sinus defect (double arrow) which in the reading reveals a suspicion

Subperiosteal abscess

In the additional evaluation of mastoid septa, the internal and external cortex of the mastoid should be examined carefully. A subperiosteal abscess has typically developed from direct extension of the inflammatory debris across the defect in the mastoid cortex.

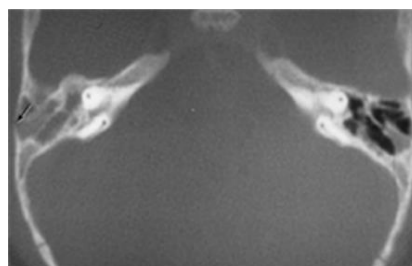


Figure 25. Coalescent otomastoiditis, subperiosteal abscess. Axial CT scan temporal showing debris that penetrated the mastoid with the mastoid septa affected when compared to the contralateral

Bezold's abscess

It is analogous to a subperiosteal abscess that occurs when the affected bone is seen at the mastoid end (instead of the external mastoid cortex) on the medial side of the insertion of digastric and sternocleidomastoid muscles. This inflammatory product extends inferiorly along the soft tissue of liver and often forms an abscess.

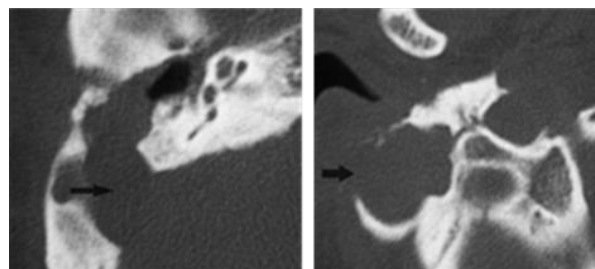


Figure 26. Mastoiditis - Bezold's abscess

Note: (a) Right temporal CT scan axial section showing mastoid debris with a large sigmoid sinus plate defect (arrow). (b) Similar cut that is inferiorly shows information on the tip of the mastoid with a large area of erosion with a large lateral bone defect (arrow).

Chronic otomastoiditis and its complications

Non-healing inflammatory process in the middle ear and mastoid associated with a period of inactivity of an inflammation. Virtually, all patients have a prolonged stage of Eustachian tube dysfunction and decreased intratympanic pressure which is the basis for precipitating factors in various disease processes (Swartz & Harnsberger 1998).

Middle ear effusion

Unexplained middle ear effusions are thought to be associated with invasion of eustachian tube lesions and tensor veli palatini. Trotter's syndrome (unilateral

deafness, pain in the trigeminal nerve and soft tissue of the stiff palate) can form if invasion affects peripheral nerves.

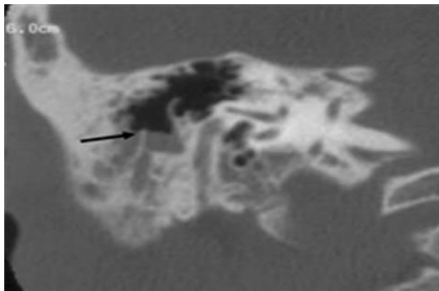


Figure 27. Middle ear effusion. Potential coronal CT scan right temporal showing multiple air fluid levels (arrows)

Inner ear

Labyrinthitis

There are various variations that cause labyrinthitis. The most common symptoms are SNHL (sensorineural hearing loss) and vertigo which may recur. Labyrinthitis has been classified in various ways, one of which is listed in the following table.

Table 2. Classification of labyrinthitis

Deployment Route	Causes	Others	
Tympanogenic	Viral	Serous	Toxic
Meningogenic	Autoimmune	Suppurative	Epidemic
Hematogenic	Bacterial		
Posttraumatic	Luetic		

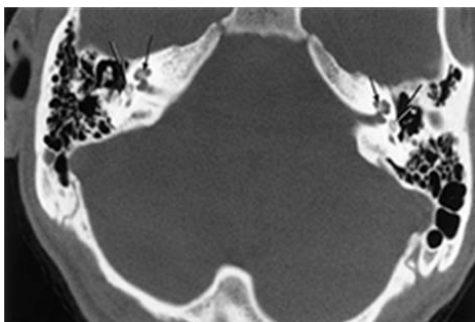


Figure 28. Labyrinth (*meningogenic*) ossification. Temporal axial CT scan section showed clear hardening in the anterior chamber (thick arrow). There was a slight change in ossification at the top of the cochlea (thin arrow)

Neoplasm on CT scan of the temporal bone

Outer ear

Cholesteatoma of the outer ear

Cholesteatoma in the external auditory canal usually occurs without hearing complaints, until the abnormality is enlarged and when it occurs, it will be accompanied by conductive deafness. Advanced cholesteatoma growth can invade mesenchymal tissue with the accumulation of necrotic debris and bone erosion in the form of a bone sequester.

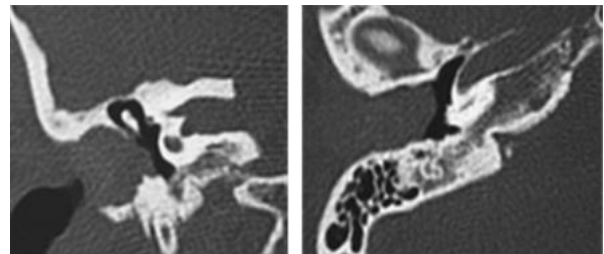


Figure 29. (a) coronal cut CT scan of the right temporal showed a large cholesteatoma filling the external auditory canal and eroding its superior and inferior walls. (b) axial-cut temporal CT scan in the same patient showed expansion of mass and pushes the tympanic tube into the middle ear space

Keratosi obturans

Keratosi obturans can be evaluated best with a CT scan, which shows remodeling or bone changes resulting in diffuse dilation of the external auditory canal.

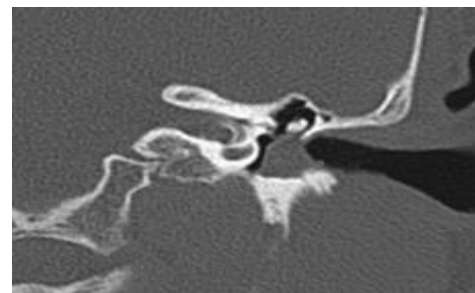


Figure 30. Coronal CT scan of the left temporal showed a soft tissue mass (*keratosi obturans*) in the fundus of external auditory canal and producing several indentations at the base of canal

Polyps

It is said that the incidence of polyps is quite high (52%) with cholesteatoma as an underlying disease, therefore temporal CT scan is useful to determine the extent of the disease and plan of action (Swartz & Harnsberger 1998).

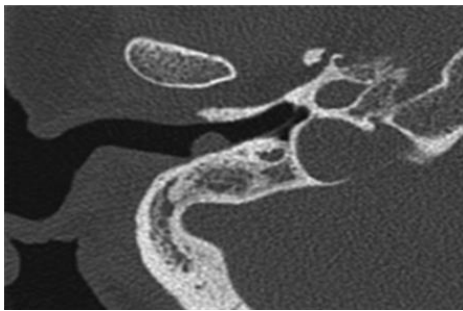


Figure 31. The right temporal axillary CT scan section revealed a small, round polyp in the exposed external auditory canal

Lipoma

Clinically, lipoma is enveloped by epithelium and by physical examination. It is somewhat unclear to diagnose it. The differential diagnosis includes angiomyolipoma. Liposarcoma showed bone erosion on temporal CT scan.

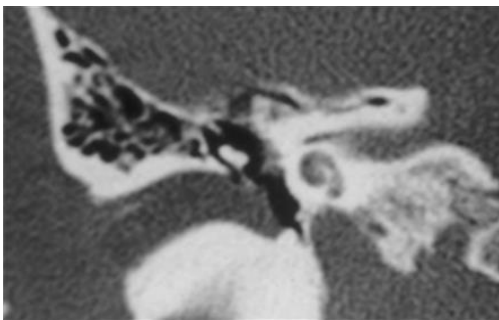


Figure 32. Coronal cut CT scan of the right temporal showed a mass in the external auditory canal, although examination using a bone window setting, the presence of a low density indicated fat direction

Arteriovenous malformations

The outer ear is the most common location for AVMs outside the head and neck. A study concluded about 44 lesions that showed an enlarged development could occur during childhood, adolescence, pregnancy and adulthood (Aspestrand & Kolbenstvedt 1995).

Tumors originating from glands

These tumors grew from cerumen glands or salivary ectopic tissue, usually appeared at age 30 to 60 years and produced otorrhea and hearing loss without pain. On physical examination, a soft tissue mass appeared in the external auditory canal without bone erosion.

Neurofibroma and schwannoma

Schwannomas arising from external auditory canal are very rare (reference). Yet, there are those that involve external auditory canal indirectly, namely schwannomas arising from cranial nerves VII and IX.

Meningioma

Meningiomas most commonly arise from intracranial and spread to the temporal bone and external auditory canal rather than arise from the temporal bone itself. In general, as much as 20% of meningiomas can spread extracranial and occur in the temporal bone. The involvement of the temporal bone in the meningioma can be evaluated with a CT scan.

Exostosis

Most exostoses are found in individuals who have been exposed to cold water frequently. This causes a bone hyperplasia reaction due to exposure to cold water. These lesions consist of a more superficial layer of bone with a denser base layer of bone that has lost vascularization.

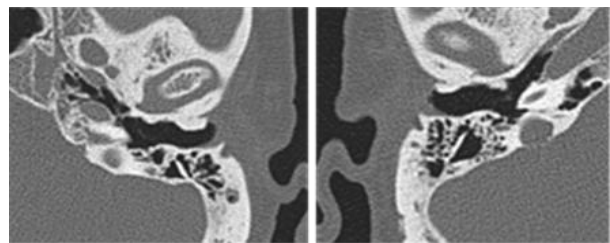


Figure 33. (a) Shaped axial CT scan of the right temporal showing coincidence, exostotic bone, small size in the anterior wall and deeper than the external auditory canal. (b) A left temporal axial CT scan revealed a large bony exostosis on the lateral side of the external auditory canal

Osteoma

CT scan with bone algorithms can help describe in detail the location and plan of surgery.

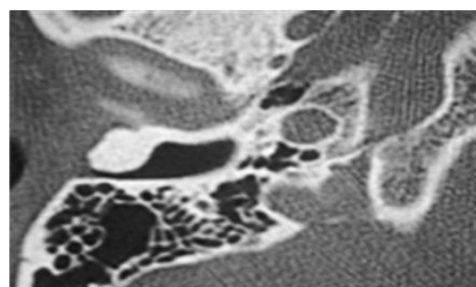


Figure 34. Axial cut CT scan of the right temporal showing a more dense osteoma involving the lateral aspect of the external auditory canal and causing significant narrowing

Carcioma

Squamous cell malignancy has been made in stages called the Pittsburgh Staging Criteria, and has undergone following modifications.

T1 : Only in the external auditory canal, without

any erosion of the bone or soft tissue involved.

- T2 : Only in the auditory canal, accompanied by bone erosion (almost the entire thickness of the bone) or soft tissue mass <0.5 cm.
- T3 : Erosion of all bone thickness or soft tissue mass <0.5 cm, involving the middle ear or mastoid.
- T4 : Involves the cochlea, petrous apex, middle ear wall, carotid canal, jugular foramen, dural, temporomandibular joint, or styloid: facial paresis and soft tissue mass > 0.5 cm.

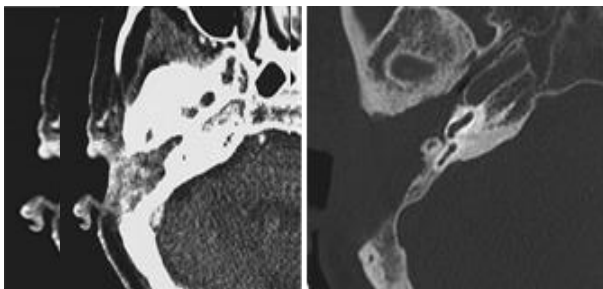


Figure 35. (a) right temporal axial CT scan with soft tissue algorithm showed a non-specific mass. (b) bone algorithm showed that the aggressiveness of mass erodes the mastoid bone and extended to the middle ear

Tumor extension can also pass through the Santorini fissure to the parotid gland and the TMJ, also across the tympanomastoid suture line to the mastoid bone and through infratemporal fossa to the face.

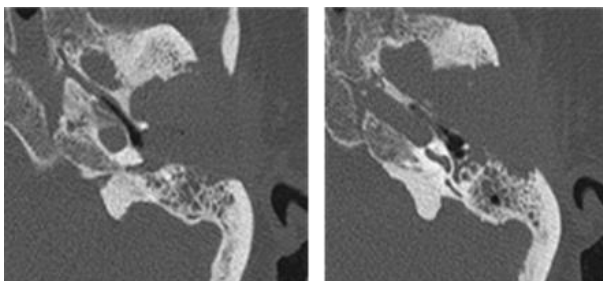


Figure 36. (a) axial cut CT scan of the left temporal showing an adenocarcinoma-like appearance of the left external auditory canal significantly eroding the skull base in the TMJ and mastoid region. (b) axial cut temporal CT scan similar to a lower level shows invasion into the middle ear

Middle ear

Cholesteatoma of the middle ear and its complications

In fact, cholesteatoma is an inaccurate name, because this lesion is not a neoplasm and can with or without cholesterol crystals, cholesteatoma can be congenital (epidermoid) (Johnson et al. 1983).

Table 3. Middle ear cholesteatoma

	%
Congenital	2
Obtain	98
Pars flaccida, (primer)	82
Pars tensa, (sekunder)	18
Posterosuperior (sinus cholesteatoma)	78
Anterior and inferior	22

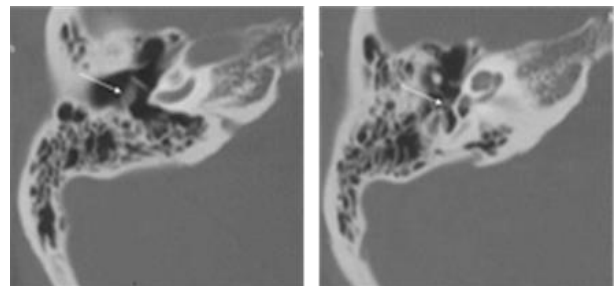


Figure 37. Cholesteatoma pars flaccida

Note: (a) axial cut CT scan of right temporal showed Prussak's space soft tissue lesion (arrow). (b) coronal cut CT scan of right temporal showed aural polyp (white arrow) and scutum erosion (black arrow). Coincidentally, it is superior to the malleal ligament (white arrow). Acquired cholesteatoma, pars tensa, (c) axial cut CT scan right temporal showed small soft tissue mass (arrow), and (d) axial cut temporal CT scan with superior cut, confirming mass attached to pyramidal surface.

In the future, if cholesteatoma is not treated properly, there will be various complications associated with bone erosion. Although the pathogenesis of bone damage remains controversial. The factors involved are mechanical, biomechanical and cellular level. Yet, there is a simple concept of a pressure mechanism that causes a direct effect of keratin expansion and is associated with debris. This tendency for bone erosion leads to changes in the middle ear cleft associated with cholesteatoma complications, namely ossicle erosion, labyrinthine fistula, involvement of facial nerve canal, expansion of petrous apex, total deafness and automastoidectomy.

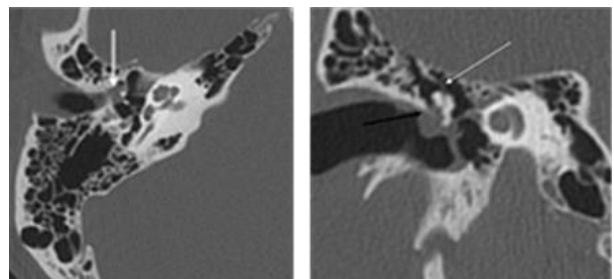


Figure 38. Cholesteatoma obtained in middle ear

Note: (a) axial section CT scan of the right temporal showing a scattered attic-antral mass which has eroded the incus body (white arrow). The lateral cortex of the semicircular canal is intact (double black arrows). (b) coronal cut CT scan of the right temporal shows changes in the attic due to cholesteatoma (double black arrows), the scutum is still intact (white arrow). Obtained Cholesteatoma, fistula labyrinth (a) axial section (b) coronal section CT scan of the right temporal showing a holotympani mass with erosions in the lateral semicircular canal cortex (arrow), indicating impending fistulation. This should be reported for the clinician's reference, noting that it is more anterior to the sigmoid sinus (S).

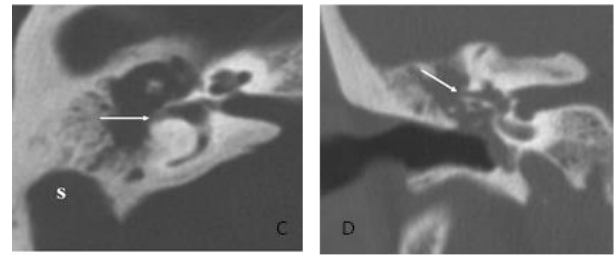


Figure 41. Middle ear schwannoma

Paraganglioma

Paraganglioma usually grows from the glomus of the body associated with the tympanic branch of the glossopharyngeal nerve (Swartz and Harnsberger, 1998).

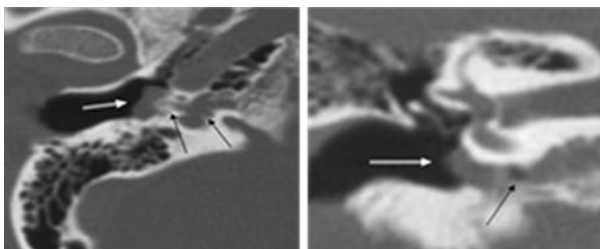


Figure 39. Paraganglioma (*glomus tympanicum*) (a) axial section (b) coronal section CT scan right temporal showing a mass with an even edge along the surface of the promontorium (white arrow), noted sublabryrin infiltration (black arrow)

Congenital cholesteatoma

In general, congenital cholesteatoma has a thinner and flatter matrix when it lies directly on intact tympanic membrane (due to pressure effects). Congenital cholesteatoma is more often unilateral, but bilateral cases have also been reported.

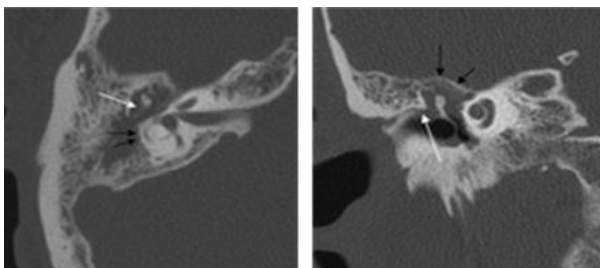


Figure 40. *Congenital cholesteatoma* (a) axial section (b) coronal section CT scan of left temporal showed soft tissue mass anterior to the tympanic space (arrow) recorded normal incudostapedial articulation (white arrow in image a) and lateral malleal ligament (white arrow in image b)

Schwannoma

There is a lack of CT compared to MRI which can differ between paraganglioma and schwannoma. It is important to know that schwannoma in the middle ear occurs more often without facial nerve palsy. The schwannoma is usually well coiled and arises from the main trunk of the facial nerve.

Rhabdomyosarcoma

In this case, CT examination helps to demonstrate the extent of destruction of bone with the use of contrast. It will help to predict more associated forms of cholesteatoma (Swartz & Harnsberger 1998).

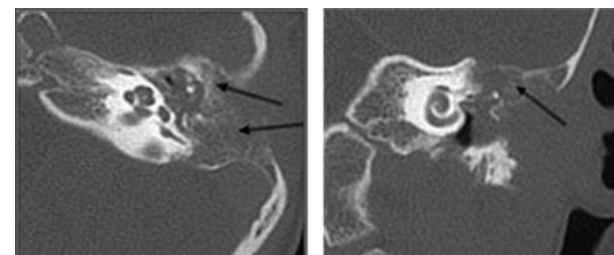


Figure 42. *Rhabdomyosarcoma*

Note: (a) Axial cut, (b) coronal cut left temporal CT scan showed middle ear mass with permeative type bone destruction.

Giant cell tumor

GCT is a very rare lesion of the temporal bone, which can extend to the middle ear and infratemporal fossa and tends to be quite large (Swartz & Harnsberger 1998).

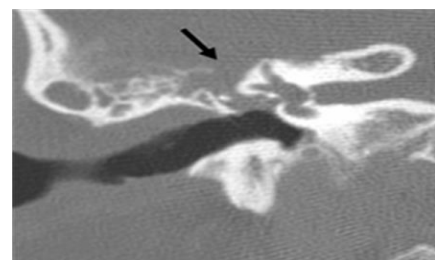


Figure 43. Giant cell tumor coronal cut right temporal CT scan. Soft tissue lesions appear in the attic and tegmental air cells with the distribution of damage to tympani tegmen (arrow)

Inner ear

Intralabyrin schwannoma

Intralabyrin schwannoma is rare, can occur occasionally and is more frequent in patients with NF-2, but most cases are more sporadic. There is a drawback to examining a CT scan rather than an MRI to look for structural abnormalities in the soft tissue.

Table 4. Intralabyrinthine schwannoma origin grouping

Based on location on the labyrinth	IAC involvement	Middle ear involvement
Intracochlear	Transmodiolar (cochlea and IAC)	Transotic (Middle ear, labyrinth, and IAC)
Intravestibular	Transmacular (vestibule and IAC)	Tympanic Labyrinthine (Middle ear and labyrinth)
Intravestibulocochlear		

Source: Kennedy RJ et al (2004)

Fibrous dysplasia

Pagetoid, sclerotic and cystic are depictable forms of fibrous dysplasia and these disorders are adequately described by temporal CT scan.

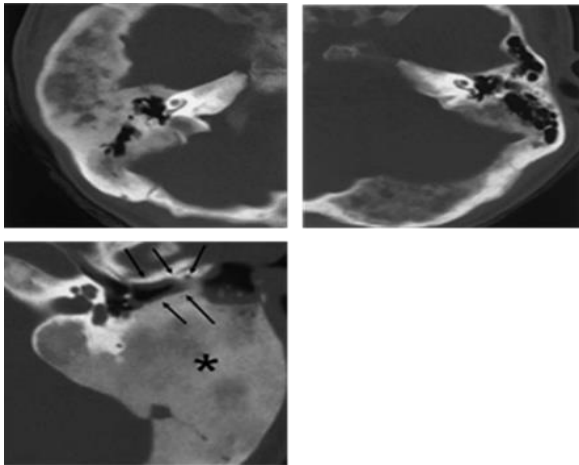


Figure 47. Fibrous dysplasia, pagetoid (a) axial cut CT scan right temporal, (b) axial CT scan left temporal, showed widespread heterogeneous thickening of the squamous and petrous temporal bone, (c) fibrous dysplasia, sclerotic. Extensive sclerotic appearance of the mastoid is characterized by increased bone volume (*). Changes in occlusion of external auditory canal were noted, often with arrow-pointed abnormalities

Strength and limitation

HRCT offers high resolution images of the temporal bone, providing detailed information on the structure and soft tissue components. Soft tissue evaluation is easier to analyze compared to MRI. HRCT protocol for temporal bone allows for easier analysis and identification of standard structures, congenital abnormalities, and pathological problems. HRCT can expose patients to radiation, which can be harmful in high doses. Tilted image reconstruction can introduce artifacts that may affect the accuracy of the images. HRCT may not be suitable for patients with certain medical conditions, such as pregnancy or kidney problems, due to the use of contrast agents. HRCT is not suitable for assessing some soft tissue structures, such as the meninges or blood vessels, which may require MRI or other imaging modalities.

CONCLUSION

There were so many and detailed potential abnormalities that occurred in the temporal bone. Its constituent structures had made a prospective radiologist forced to be more observant and thorough in evaluating the area, with the guidance and sample images obtained. It was expected that it could help prospective radiologists to describe structural abnormalities.

Acknowledgment

The authors would like to Department of Radiology, Faculty of Medicine, Universitas Airlangga/ Dr. Soetomo General Academic Hospital, Surabaya, Indonesia

Conflict of interest

None0

Funding disclosure

None.

Author contribution

WF and IBGR were conceptual idea, study design, collected data. BGR was write and revised the manuscript. WF was analysis data, checking grammar, and validation the manuscript to publish.

REFERENCES

- Aspestrand F, Kolbenstvedt A (1995). Vascular mass lesions and hypervascular tumors in the head and neck: Characteristics at CT, MR imaging and angiography. *Acta radiol* 36, 136–141.
- Chandrasekhar S, De la Cruz A, Garrido E (1995). Surgery of congenital aural atresia. *Am J Otol* 16, 713–717.
- Graham J, Phelps P, Michaels L (2000). Congenital malformations of the ear and cochlear implantation in children: Review and temporal bone report of common cavity. *J Laryngol Otol Suppl* 25, 1–14.
- Hasso A, Casselman J, Broadwell R (1996). Temporal bone congenital anomalies. In: *Head and Neck Imaging*. Mosby, St. Louis (MO).
- Hasso A, Vignaud J, Desmedt E (1989). Normal anatomy and pathology of the temporal bone and mastoid. In: *Computed Tomography of the Head and Neck*. Raven Press, New York.
- Howard J, Elster A, May J (1990). Temporal bone: Three-dimensional CT. Part II. Pathologic alterations. *Radiology* 177, 427–430.

- Johnson D, Voorhees R, Lufkin R (1983). Cholesteatomas of the temporal bone: Role of CT. *Radiology* 148, 733–737.
- Kennedy R, Shelton C, Salzman K, et al (2004). Intralabyrinthine schwannomas: diagnosis, management, and a new classification system. *Otol Neurotol* 25, 160–167.
- Koßling S, Omenzetter M, Bartel-Friedrich S (2009). Congenital malformations of the external and middle ear. *Eur J Radiol* 69, 269–279.
- Mayer T, Brueckmann H, Siegert R (1997). High-resolution CT of the temporal bone in dysplasia of the auricle and external auditory canal. *AJNR Am J Neuroradiol* 18, 53–65.
- McCullough C, Zink F (1999). Performance evaluation of a multi-slice CT system. *Med Phys* 26, 2223–2230.
- McElveen JJ, Carrasco V, Miyamoto R (1997). Cochlear implantation in common cavity malformations using a transmastoid labyrinthotomy approach. *Laryngoscope* 107, 1032–1036.
- Park A, Kou B, Hotaling A (2000). Clinical course of pediatric congenital inner ear malformations. *Laryngoscope* 110, 1715–1719.
- Phelps P, Reardon W, Pembrey M (1991). X-linked deafness, stapes gushers and a distinctive defect of the inner ear. *Neuroradiology* 33, 326–330.
- Propst E, Blaser S, Gordon K (2005). Temporalbone findings on computed tomography imaging in branchio-oto-renal syndrome. *Laryngoscope* 115, 1855–1862.
- Quirk B, Youssef A, Ganau M, et al (2019). Radiological diagnosis of the inner ear malformations in children with sensorineural hearing loss. *BJR Open* 1, 2–8.
- Sennaroglu L, Saatci I (2002). A new classification for cochleovestibular malformations. *Laryngoscope* 112, 2230–2241.
- Shaffer K, Haughton V, Wilson C (1980). High resolution computed tomography of the temporal bone. *Radiology* 134, 409–414.
- Swartz J, Harnsberger K (1998). *Imaging of the temporalbone*. Thieme, New York.
- Torizuka T, Hayakawa H (1992). High-resolution CT of the temporal bone: A modified baseline. *Radiology* 184, 109–111.
- Weerden H (1988). Classification of congenital deformities of the auricle. *Facial Plast Surg* 5, 385–388.
- Yalcin S, Karlidag T, Kaygusuz I, et al (2003). Firstbranchial cleft sinus presenting with cholesteatoma and external auditory canal atresia. *Int J Pediatr Otorhinolaryngol* 67, 811–814.